

# FTIR

## TALK LETTER

Vol. 39



Catalytic Nitrogen Fixation under Mild Reaction  
Conditions Using Base Metal-Dinitrogen Complexes — 02

Regulatory Compliance for Infrared Microscopes — 06

Using Derivative Spectra — 10

Q&A What measurement method should I use  
to check the degradation of lubricant oil? — 15

Integrated EDX-FTIR Analysis Software "EDXIR-Analysis"  
Advanced Performance UniBloc Balances  
"AP W-AD Series" — 16

# Catalytic Nitrogen Fixation under Mild Reaction Conditions Using Base Metal-Dinitrogen Complexes



Department of Applied Chemistry, School of Engineering, The University of Tokyo  
Shogo Kuriyama, Research Associate

## 1. Introduction

Ammonia serves as a source of nitrogen for the DNA and proteins that made up living organisms and is a raw material for various nitrogen-containing chemical products. Ammonia has also attracted recent interest as a potential decarbonized fuel due to the ease of producing liquid ammonia, high energy density, and no carbon dioxide emissions upon combustion. Ammonia is synthesized from molecular nitrogen (dinitrogen), which makes up approx. 80 % of atmospheric gas, but due to its very strong N≡N triple bond, reducing dinitrogen into ammonia involves an extremely difficult chemical reaction termed nitrogen fixation.

Industrially, nitrogen fixation is performed using the Haber-Bosch process developed 100 years ago (Fig. 1 (a)). The Haber-Bosch process uses solid iron-based catalysts to synthesize ammonia by reacting nitrogen gas and hydrogen gas at high temperatures and pressures. The hydrogen gas used in this reaction is produced by fossil fuel reforming, a process that emits carbon dioxide and requires large amounts of energy. Ideally, a novel method of nitrogen fixation is needed that can synthesize ammonia under mild reaction conditions without being dependent on fossil fuels.

In nature, dinitrogen in the atmosphere is converted into ammonia under ambient pressures and temperatures by the nitrogen-fixing enzyme nitrogenase (Fig. 1 (b)). Studies have revealed the nitrogenase active site has a sulfur-bridged iron-molybdenum cluster structure with a carbon atom center. For many years, research into methods of nitrogen fixation under mild conditions has attempted to mimic the active center of nitrogenase by using nitrogen complexes of transition metals that coordinate dinitrogen at the transition metal center. The first catalytic methods of ammonia formation using transition metal complexes were reported in 2003 by Schrock et al. and used molybdenum-dinitrogen complexes as catalysts.<sup>[1]</sup> In the intervening years, numerous research groups have successfully

formed ammonia catalytically using various transition metal catalysts.<sup>[2]</sup>

Our laboratory has reported the catalytic formation of ammonia using molybdenum-dinitrogen complexes with tridentate pincer ligands (Fig. 1 (c)).<sup>[3,4]</sup> We have also reported the catalytic formation of ammonia using mainly molybdenum and various other transition metal-dinitrogen complexes.<sup>[5]</sup> This article describes our recent use of base metal dinitrogen complexes with iron and cobalt to achieve catalytic nitrogen fixation.<sup>[6,7]</sup>

When dinitrogen coordinates to metal, in addition to the usual  $\sigma$  donation, there is a reduction in bond order due to back donation from the occupied d orbital of the metal to the  $\pi^*$  orbital of the dinitrogen (Fig. 1 (d)). The stretching vibration of free dinitrogen is observed at 2331  $\text{cm}^{-1}$ , but coordination shifts this frequency to a lower wavenumber. The stretching vibration of the terminal dinitrogen in a transition metal complex is infrared active, and the degree of activation of the dinitrogen can be quantified by measuring its infrared absorption. The number of coordinated dinitrogens and their coordination mode can also be determined based on the absorption pattern of stretching vibrations recorded in an infrared spectrum. However, while infrared spectral analysis is essential for the synthesis of transition metal-dinitrogen complexes, transition metal-dinitrogen complexes are often sensitive to air and water. Infrared spectra are frequently measured with KBr pellets or in a solvated state with an organic solvent, but avoiding contact with air and water during sample preparation and spectral measurement poses a serious challenge. A simple method of measuring the infrared spectra of highly reactive complexes while avoiding these challenges was devised by installing an IRSpirit device in a glove box.

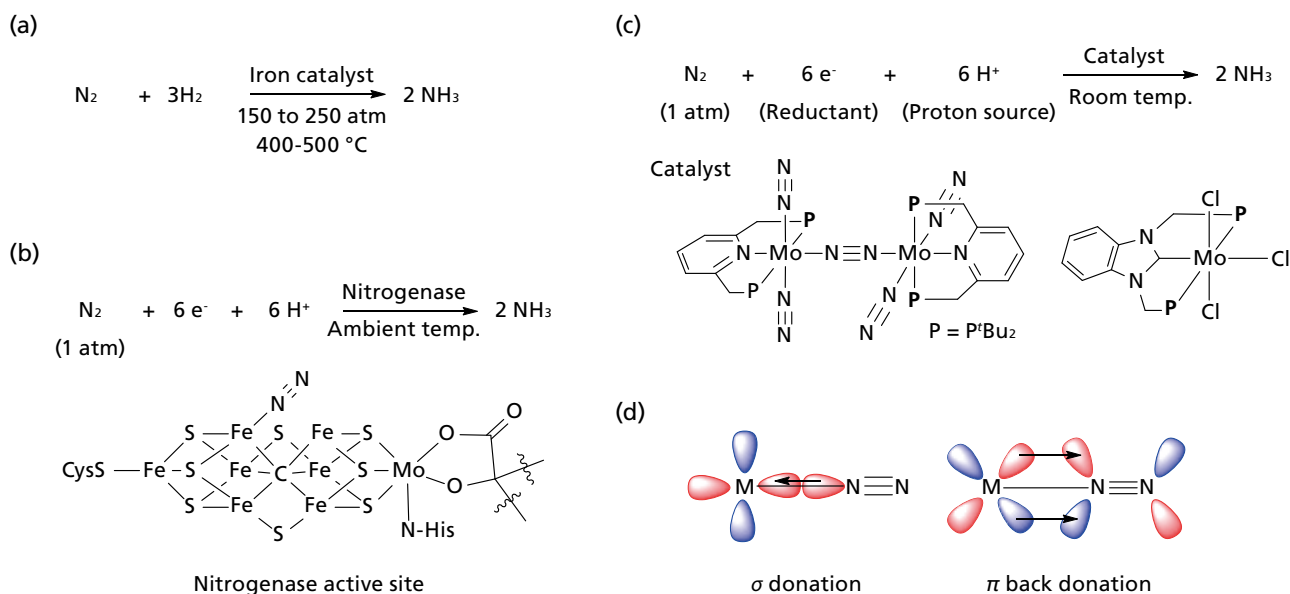


Fig. 1 (a) Haber-Bosch Process (b) Nitrogenase (c) Nitrogen Fixation Using Transition Metal Complex (d) Dinitrogen Coordination

## 2. Catalytic Synthesis of Ammonia and Hydrazine from Dinitrogen Using Iron Complexes

Although the nitrogenase active site is known to have a cluster structure with iron-carbon bonds, the detailed mechanism of action of the active site is unknown. Recent research suggests that dinitrogen is coordinated to a carbon-coordinated iron center (Fig. 1 (b)). This finding sparked interest in studying the reactivity of iron-dinitrogen complexes with iron-carbon bonds as potential models of nitrogenases. We devised an iron complex catalyst with an anionic PCP-type pincer ligand and benzene backbone that has strong electron-donating properties and coordinates strongly with metals.<sup>[6]</sup>

An iron(I)-dinitrogen complex with a PCP-type pincer ligand was synthesized as shown in Fig. 2 (a) (complex 1). The infrared spectrum of complex 1 shows absorption at 1954  $\text{cm}^{-1}$  attributable to a terminal dinitrogen ligand. Next, we used this iron complex to investigate the catalytic reduction of dinitrogen. In the presence of a catalytic amount of complex 1, nitrogen gas at ambient pressure was reacted with potassium graphite ( $\text{KC}_8$ ) as a reductant and oxonium salt ( $[\text{H}(\text{OEt})_2]\text{BAr}^{\text{F}}_4$ ,  $\text{Ar}^{\text{F}} = 3,5\text{-(CF}_3)_2\text{C}_6\text{H}_3$ ) as a proton source at  $-78\text{ }^\circ\text{C}$  in diethyl ether. The reaction produced 252 equiv. of ammonia, 68 equiv. of hydrazine, and fixed up to 388 equiv. of dinitrogen per catalyst. This yield was higher than any other iron catalyst, and showed this complex has the highest catalytic activity of any iron catalyst for nitrogen fixation.

The iron complex was then reduced to gain insight into the reaction mechanism (Fig. 2 (b)). Using potassium to perform the single-electron reduction of complex 1 in a nitrogen atmosphere resulted in two new absorption bands attributable to terminal nitrogen ligands at 1981  $\text{cm}^{-1}$  and 1894  $\text{cm}^{-1}$  in addition to absorption by the starting material (Fig. 2 (c)). This suggested that reduction produced a complex with two dinitrogens coordinated at the iron center in cis orientation. Finally, single-crystal X-ray structure analysis determined the complex to be an anionic iron(0)-dinitrogen complex (2). Because this anionic complex was catalytically active, this iron(0)-dinitrogen complex is likely to be the active form of the complex that generated ammonia and hydrazine.

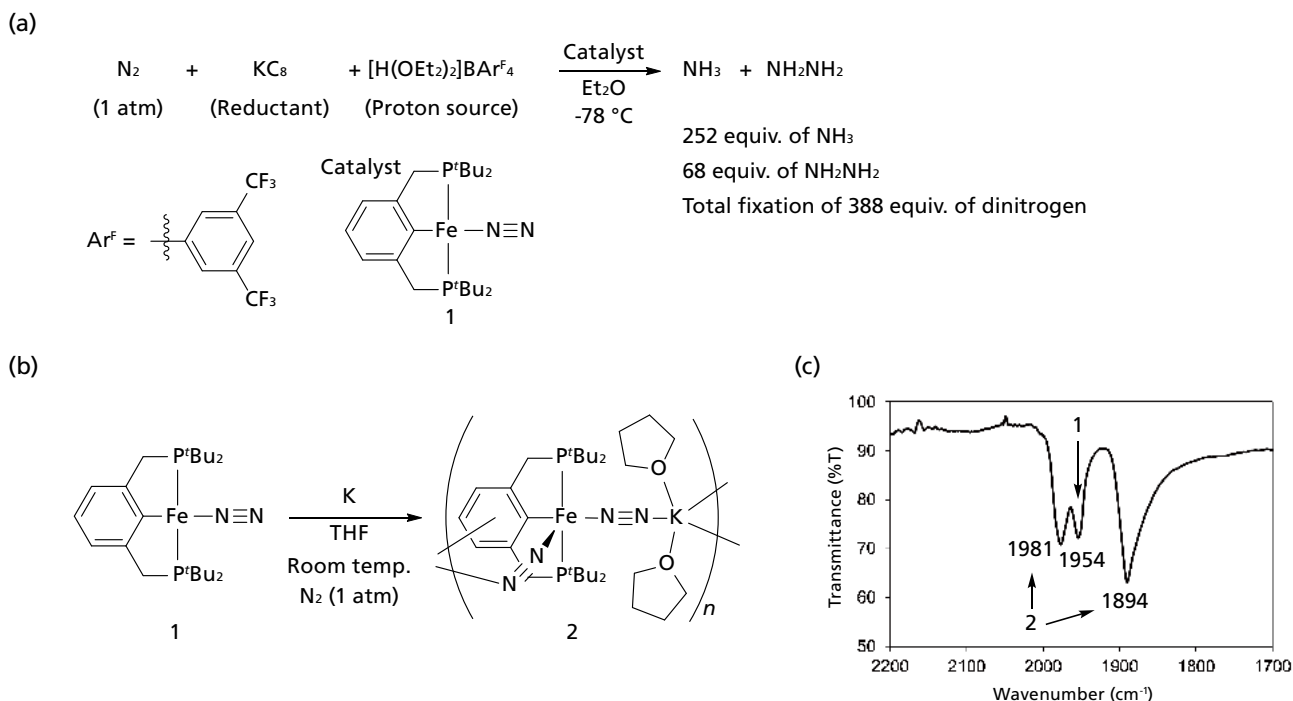


Fig. 2 (a) Ammonia and Hydrazine Formation from Dinitrogen Using an Iron-Dinitrogen Complex  
(b) Reduction of Iron-Dinitrogen Complex  
(c) Infrared Spectrum of Reduced Iron-Dinitrogen Complex

### 3. Catalytic Formation of Silylamine from Dinitrogen Using a Cobalt Complex

Silylamine ( $\text{N}(\text{SiMe}_3)_3$ ) is readily converted into ammonia by hydrolysis, hence the synthesis of silylamine from dinitrogen is frequently studied as a model for ammonia synthesis and an example of nitrogen fixation. To date, various transition metal-dinitrogen complexes have been reported to catalyze silylamine formation, of which cobalt complexes are shown to be highly active.<sup>[8]</sup>

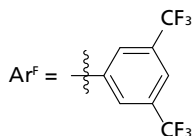
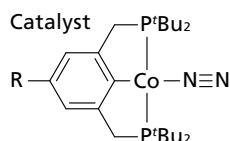
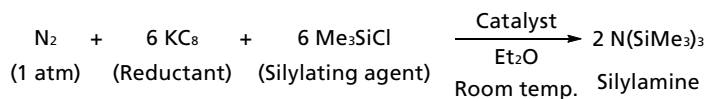
Our laboratory has reported on group 9 rhodium- and iridium-dinitrogen complexes bearing an anionic pincer ligand that catalyze silylamine formation.<sup>[9,10]</sup> Based on these findings, we inferred that silylamine formation could be similarly catalyzed by a homologous cobalt complex bearing an anionic pincer ligand.<sup>[7]</sup>

Cobalt-dinitrogen complexes with anionic PCP-type pincer ligands were synthesized. Complexes with substituents on the benzene ring of the pincer ligand were also synthesized to investigate the impact of the electronic properties of these substituents. The infrared spectrum of unsubstituted complex **3** showed absorption by coordinated dinitrogen at  $2009 \text{ cm}^{-1}$ . This absorption shifted to a lower wavenumber in complexes **4** and **5** that bore electron-donating methoxy (OMe) and *tert*-butyl (*t*Bu) groups ( $2005$  and  $2006 \text{ cm}^{-1}$ , respectively), suggesting the dinitrogen was more highly activated due to increased back

donation from the cobalt center to the coordinated dinitrogen. By contrast, absorption shifted to a higher wavenumber in complex **6** that bore an electron-withdrawing 3,5-bis(trifluoromethyl)phenyl ( $\text{Ar}^{\text{F}}$ ) group ( $2014 \text{ cm}^{-1}$ ), indicating reduced back donation.

These complexes were then used to catalyze the formation of silylamine. Using unsubstituted complex **3** as the catalyst and reacting nitrogen gas at ambient pressure with potassium graphite as a reductant and trimethylchlorosilane as a silylating agent in THF at room temperature for 96 hours yielded 351 equiv. of silylamine per catalyst. This was a higher catalytic activity than any previously reported catalyst. Using complexes **4** and **5** that bear electron-donating substituents yielded 332 and 371 equiv. of silylamine, respectively, showing catalytic activity almost equivalent to unsubstituted complex **3**. By contrast, complex **6** that bears an electron-withdrawing substituent yielded just 106 equiv. of silylamine. The reduced catalytic activity was probably due to weakened back donation to the coordinated dinitrogen caused by the substituted electron-withdrawing group that left the dinitrogen less highly activated. In summary, the newly synthesized cobalt complexes were shown to be the most active catalysts of silylamine formation to date.

(a)



| Catalyst | R               | $\nu_{\text{NN}}$<br>( $\text{cm}^{-1}$ ) | $\text{N}(\text{SiMe}_3)_3$<br>(equiv.) |
|----------|-----------------|---|---|
| 3        | H               | 2009                                      | 351                                     |
| 4        | OMe             | 2005                                      | 332                                     |
| 5        | <sup>t</sup> Bu | 2006                                      | 371                                     |
| 6        | Ar <sup>F</sup> | 2014                                      | 106                                     |

(b)

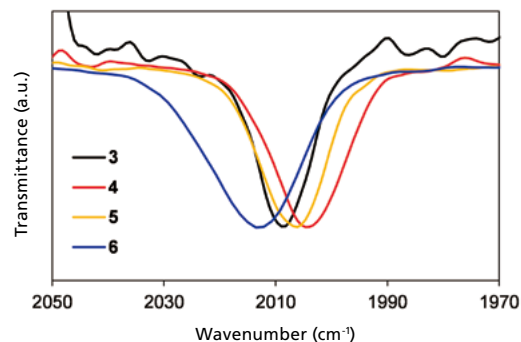


Fig. 3 (a) Formation of Silylamine from Dinitrogen Using Cobalt-Dinitrogen Complexes  
(b) Infrared Spectra of Cobalt-Dinitrogen Complexes

## 4. Conclusion

The research described in this article shows that base metal complexes with anionic PCP-type pincer ligands are efficient catalysts of nitrogen fixation under mild conditions. We are now working on developing more environmentally friendly reaction systems by combining more active catalysts with more active electrochemical reactions.

### Acknowledgments

These findings were made under the tutelage of Professor Yoshiaki Nishibayashi. We would like to thank the members of our laboratory for their collaboration in this work. We would also like to thank the research groups of Professor Kazunari Yoshizawa at Kyushu University and Professor Hiromasa Tanaka at Daido University.

### References

- [1] D. V. Yandulov, R. R. Schrock, *Science*. **2003**, *301*, 76–78.
- [2] Y. Tanabe, Y. Nishibayashi, *Chem. Soc. Rev.* **2021**, *50*, 5201–5242.
- [3] K. Arashiba, Y. Miyake, Y. Nishibayashi, *Nat. Chem.* **2011**, *3*, 120–125.
- [4] Y. Ashida, K. Arashiba, K. Nakajima, Y. Nishibayashi, *Nature* **2019**, *568*, 536–540.
- [5] Y. Ashida, Y. Nishibayashi, *Chem. Commun.* **2021**, *57*, 1176–1189.
- [6] S. Kuriyama, T. Kato, H. Tanaka, A. Konomi, K. Yoshizawa, Y. Nishibayashi, *Bull. Chem. Soc. Jpn.* **2022**, *95*, 683–692.
- [7] S. Kuriyama, S. Wei, H. Tanaka, A. Konomi, K. Yoshizawa, Y. Nishibayashi, *Inorg. Chem.* **2022**, *61*, 5190–5195.
- [8] Y. Tanabe, Y. Nishibayashi, *Coord. Chem. Rev.* **2019**, *389*, 73–93.
- [9] R. Kawakami, S. Kuriyama, H. Tanaka, K. Arashiba, A. Konomi, K. Nakajima, K. Yoshizawa, Y. Nishibayashi, *Chem. Commun.* **2019**, *55*, 14886–14889.
- [10] R. Kawakami, S. Kuriyama, H. Tanaka, A. Konomi, K. Yoshizawa, Y. Nishibayashi, *Chem. Lett.* **2020**, *49*, 794–797.

# Regulatory Compliance for Infrared Microscopes

Spectroscopy Business Unit, Analytical & Measuring Instruments Division

Yusuke Aoi

Data integrity (DI) is now a strict requirement of regulatory authorities in the pharmaceutical industry. The scope of regulatory interest in analytical instruments is now growing to include not only chromatographic instruments such as liquid chromatographs and gas chromatographs, but also spectrometric instruments such as Fourier transform infrared (FTIR) spectrophotometers.

Shimadzu currently sells the database management and client server versions of LabSolutions (LabSolutions DB/CS) as an analytical network data system that offers DI compliance. LabSolutions DB/CS comes with functions that support DI compliance, and the FTIR spectrophotometer control and analysis software LabSolutions IR is compatible with LabSolutions DB/CS.

While confirmation testing performed on an FTIR spectrophotometer requires DI compliance, DI compliance is not required for the analysis of minute contaminants on an

infrared (IR) microscopy system. Nevertheless, IR microscopy systems that are used to analyze contaminants are often installed in the same laboratories as instruments used for confirmation testing, and when undergoing inspection the inspectors must be informed that these instruments do not comply with DI requirements. To eliminate this inconvenience, Shimadzu's AIMsolution control software for IR microscopes used in contaminant analysis now supports DI compliance. Specifically, Shimadzu has linked the AIMsolution control software with LabSolutions IR, software with a proven track record in confirmation testing, thereby leaving AIMsolution only responsible for measurements while LabSolutions IR handles the rest of the data management. This system is described in detail below. For more information on Shimadzu's AIM-9000 IR microscope, please also refer to FTIR TALK LETTER Vol. 28.

## 1. Measurement Procedure

As shown in Fig. 1, the user begins by launching and logging into the LabSolutions software with a proven track record in DI compliance. The user then selects FTIR via the instrument selection option and launches the LabSolutions IR launcher window. If AIMsolution DB/CS is installed, the AIM measurement launch button is active and can be selected to launch AIMsolution.

Once AIMsolution DB/CS is launched, it functions identical-

ly to AIMsolution (please refer to FTIR TALK LETTER Vol. 28 for more information on operating the software).

After instrument initialization, the user locates the item to be measured by controlling the wide-field camera and microscope camera in the microscope setup window. After verifying the item in the cameras, the measurement position is set on the microscope camera as shown in Fig. 2 (aperture setup).

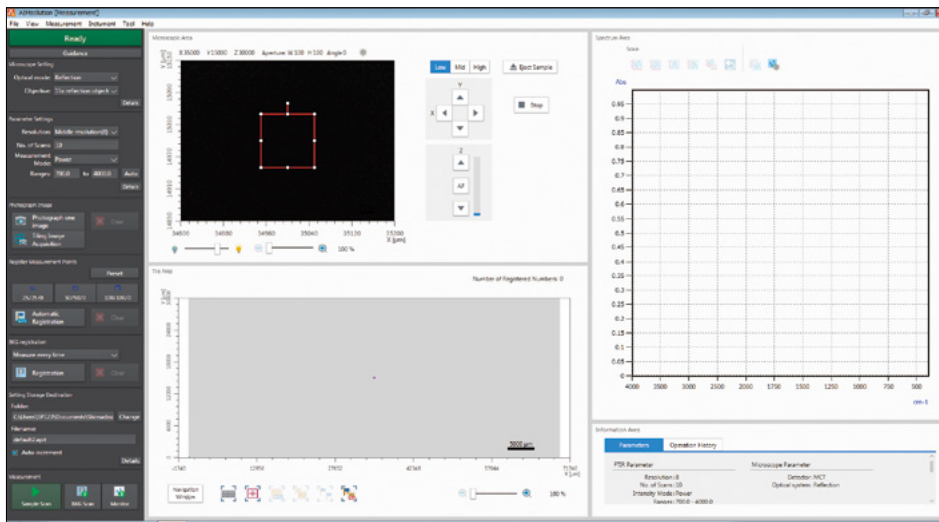
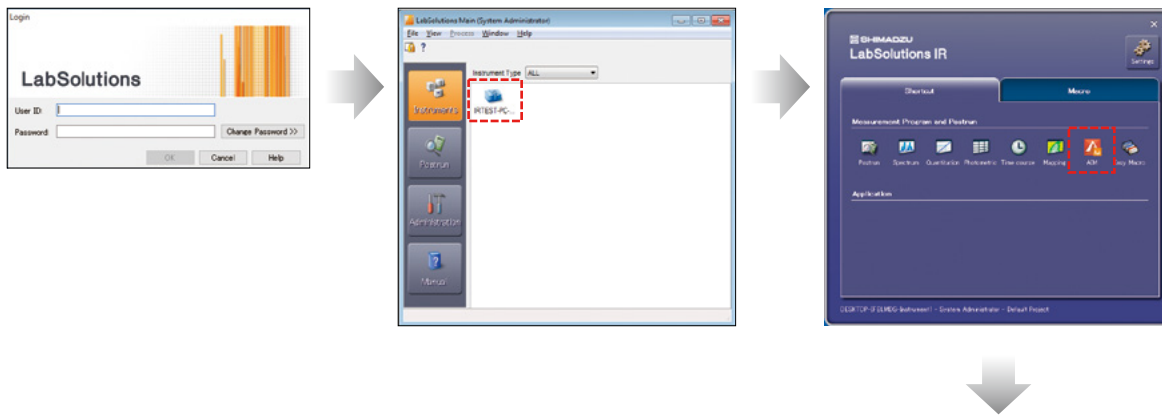


Fig. 1 AIMsolution DB/CS Startup Procedure

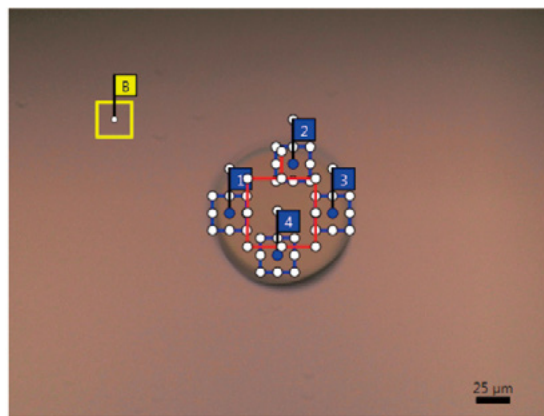


Fig. 2 Aperture Setup

Next, once the measurement parameters are set, pressing the sample measurement button begins the measurement of the IR absorption spectrum in the area that was set using the aperture. Once the spectrum measurement is complete, the image data, IR spectrum, and other data are converted to a LabSolutions IR

format and stored in the LabSolutions database. An audit trail log encompassing software startup to measurement completion is also stored in the LabSolutions database and can be viewed in the log browser.

## 2. Analytical Method

From the data imported to LabSolutions IR, the image of the registered points and the spectra at the measured points are stored in the same file as shown in Fig. 3. Because the data is

in the LabSolutions IR file format, all LabSolutions IR data processing, and search functions can be applied to the data and an audit trail log is generated of all analytical operations.

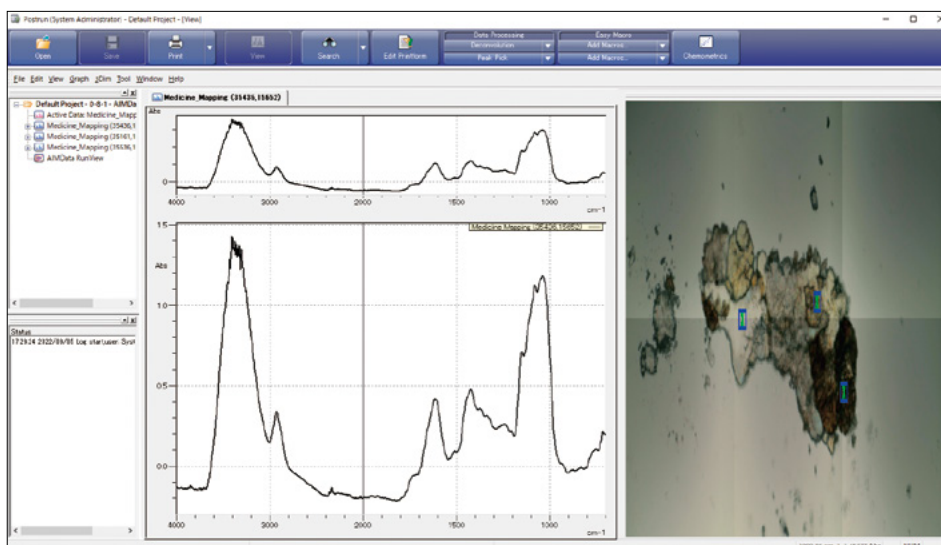


Fig. 3 IR Microscope Data Imported into LabSolutions IR

The data manager shows measurement result reports saved as PDF files and parameters as HTML files, etc., similar to data measured in LabSolutions IR. As shown in Fig. 4, executing the “Create Report Set” option in LabSolutions outputs the analysis list, log, and analysis report, all needed to ensure DI,

as a single PDF report. Furthermore, because the report set and the data are linked electronically, executing the report review and approval process electronically also automatically reviews and approves the measurement data.

**(1) Select any file.**

**Data Manager Window**

**(2) Right-click and select “Create Report Set.”**

**(3) A report set is created automatically.**

**Data Manager Window**

**Report set is combined into a single PDF file and stored in the database.**

**Analysis List**

**Log** (Data Collection (Operations) Report)

**Analysis Report**

**Measurement Parameters**

**Data History**

**Example LabSolutions DB/CS report set for spectrometric instrument**

Fig. 4 Report Set Overview

### 3. Notes

---

When using AIMsolution DB/CS, because data is managed on the LabSolutions IR database, data cannot be analyzed using the normal version of the AIMsolution analysis software. AIMsolution DB/CS also does not support AIMsolution mapping measurement.

### 4. Summary

---

As outlined above, robust regulatory compliance can be achieved for IR microscope systems by using LabSolutions DB/CS, LabSolutions IR, and AIMsolution DB/CS and employing LabSolutions features such as user management, security management, inspection of audit trail logs, file version control, and report set-based approval processes.

# Using Derivative Spectra

Solutions COE, Analytical & Measuring Instruments Division

Shoko Iwasaki

Derivative spectra are used to determine the accurate position of peaks, separate multiple peaks that are close together, calculate quantitative values, and so on. FTIR TALK LETTER Vol. 10 described the algorithms used for FTIR data processing. This article discusses derivative spectra.

## 1. Overview of Derivative Spectra

Some advantages of derivative spectra are listed below.

- (1) Wavenumbers can be confirmed for broad peaks.
- (2) Peaks can be separated even if they overlap by a slight wavenumber difference.
- (3) Shoulder peaks can be checked.
- (4) Vertical fluctuations in the baseline can be corrected.

In particular, if a peak is not caused by a single component, calculating the derivative of the spectrum can separate hidden or shoulder peaks from multiple components that appear as a single peak and determine the position of each separated peak. Derivative spectra can also be used for quantitative analysis. The principle can be explained based on the Lambert-Beer law, as expressed by equation (1).

Equation (1) and the Lambert-Beer law illustrated in Fig. 1 indicate that absorbance  $A$  is proportional to the concentration  $c$  and optical path length  $L$  of a substance. Therefore, if the optical path length is fixed, then a calibration curve can be used to calculate the concentration  $c$  of a substance from its absorbance.

Next, the derivative of equation (1) is calculated. The first derivative is expressed by equation (2) and the  $n$ th derivative by equation (3). Note that the proportional relationship between concentration  $c$  and the optical path length  $L$  remains unchanged even after differentiation. That means multiple peaks can be separated by calculating the derivative and the concentration of respective separated components can be quantitated based on peak heights and areas.

$$\text{Absorbance (Absorbance : } A) = \log(I_0/I) = \epsilon \cdot c \cdot L \quad \dots \text{ Eq. (1)}$$

$$\frac{dA}{d\lambda} = \frac{d\epsilon}{d\lambda} \cdot c \cdot L \quad \dots \text{ Eq. (2)}$$

$$\frac{d^n A}{d\lambda^n} = \frac{d^n \epsilon}{d\lambda^n} \cdot c \cdot L \quad \dots \text{ Eq. (3)}$$

$\epsilon$ : Molar absorption coefficient,  $c$ : Concentration (mol/L),  
 $L$ : Optical path length (cm),  $\lambda$ : Wavelength

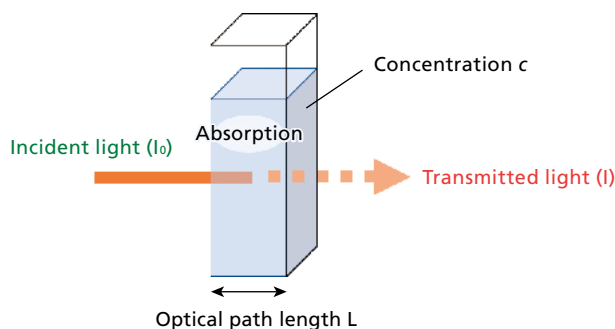


Fig. 1 Illustration of Lambert-Beer Law

Derivative spectra are typically calculated by the Savitzky-Golay method.<sup>[1, 2, 3]</sup> The method was originally developed as a spectrum smoothing technique. However, Shimadzu LabSolutions IR FTIR control software uses it for calculating derivative spectra and also smoothing.

The Savitzky-Golay method assumes that near data points sampled at equal intervals spectra can be represented by polynomial curves, with the least squares method used to determine weighting factors used for fitting the polynomial curves to the spectrum.<sup>[4]</sup> Savitzky and Golay reported a table of weighting factors for various polynomial degrees, number of smoothing points, and number of differentiation points, so that complex calculations do not need to be performed each time.

Fig. 2 shows a diagram of the smoothing procedure. In this case, seven data ranges were selected. The circle indicates a calculated data point (i) after smoothing.

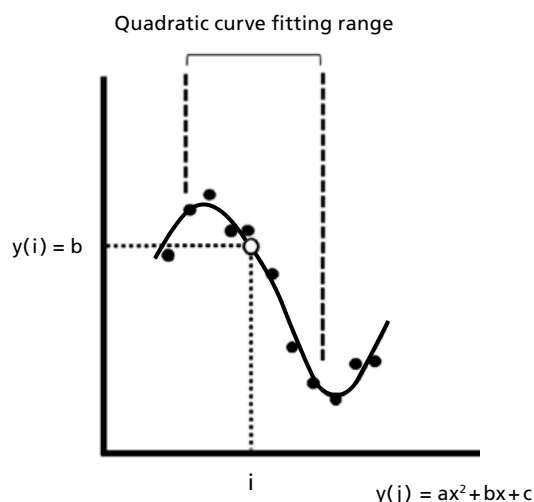


Fig. 2 Diagram of 7-Point Smoothing by Second or Third-Order Polynomial Fitting<sup>[3]</sup>

Next, it is assumed that respective points  $j$  centered around point  $i$  are expressed by Equation (4).

$$y(j) = a(j-i)^2 + b(j-i) + c \quad \dots \text{Eq. (4)}$$

$i$ : Center point;  $j$ : Respective points

Differentiation of Equation (4) results in Equation (5).

$$y'(j) = 2a(j-i) + b \quad \dots \text{Eq. (5)}$$

Since  $y'(i) = b$  at center point  $i$ , the derivative value  $y'(i)$  at center point  $i$  can be determined by determining coefficient  $b$ .

Lastly, as a precautionary point, note that the larger the number of differentiation points, the lower the noise level, but that will also decrease the peak intensity level, which results in broader peaks.<sup>[4]</sup> That means the number needs to be set based on the purpose of smoothing, while comparing the results to the original infrared spectrum. In addition, the higher the polynomial order, the closer the fit, but the less the smoothing effect will be. Consequently, typically second (or third) order polynomial fitting is used.<sup>[3]</sup> Thus, appropriate parameter settings must be specified.

## 2. Characteristics of Derivative Spectra

The characteristics of first to fourth derivative spectra are described below. For the infrared spectra from vegetable oil in Fig. 3, the corresponding first to fourth derivative spectra are shown in Fig. 4 (a) to (d). The number of differentiation points was set to 25.

Firstly, the first-order derivative spectrum is used to confirm the wavenumber of the single large peak. The wavenumbers of the zero points in the first-order derivative spectrum, where values change from positive to negative and change from negative to positive, indicate the peak and base positions. The first-order derivative spectrum in Fig. 4 (a) shows that a major peak exists where the spectrum intercepts the baseline near  $1,745 \text{ cm}^{-1}$ .

Thus, first, second, and even higher-order third and fourth-order derivative spectra are used to separate adjacent peaks or separate shoulder peaks. In Fig. 4 (a) and (c), the wavenumber of the peak position in the original spectrum is indicated by the zero points in the first and third-order derivative spectra. Meanwhile, the absorbance in the original spectrum resulted in a valley in the second-order spectrum in Fig. 4 (b) and a peak in the fourth-order derivative spectrum in Fig. 4 (d). Similarly, in case of a transmittance spectrum, a peak in the original spectrum would appear as a peak in the second-derivative spectrum and a valley

in the fourth-derivative spectrum.

Furthermore, the higher the order, the narrower the FWHM values will be in derivative spectra. Consequently, closely adjacent or shoulder peaks can be separated by calculating higher-order derivative spectra. The appropriate order level of derivative spectra should be determined by observing the status of peak separation. Though LabSolutions IR only supports first to fourth-order differentiation, it can be repeated to calculate higher-order derivative spectra.

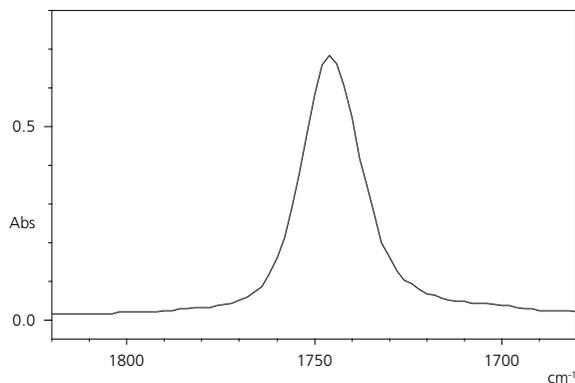


Fig. 3 Infrared Spectrum of Vegetable Oil

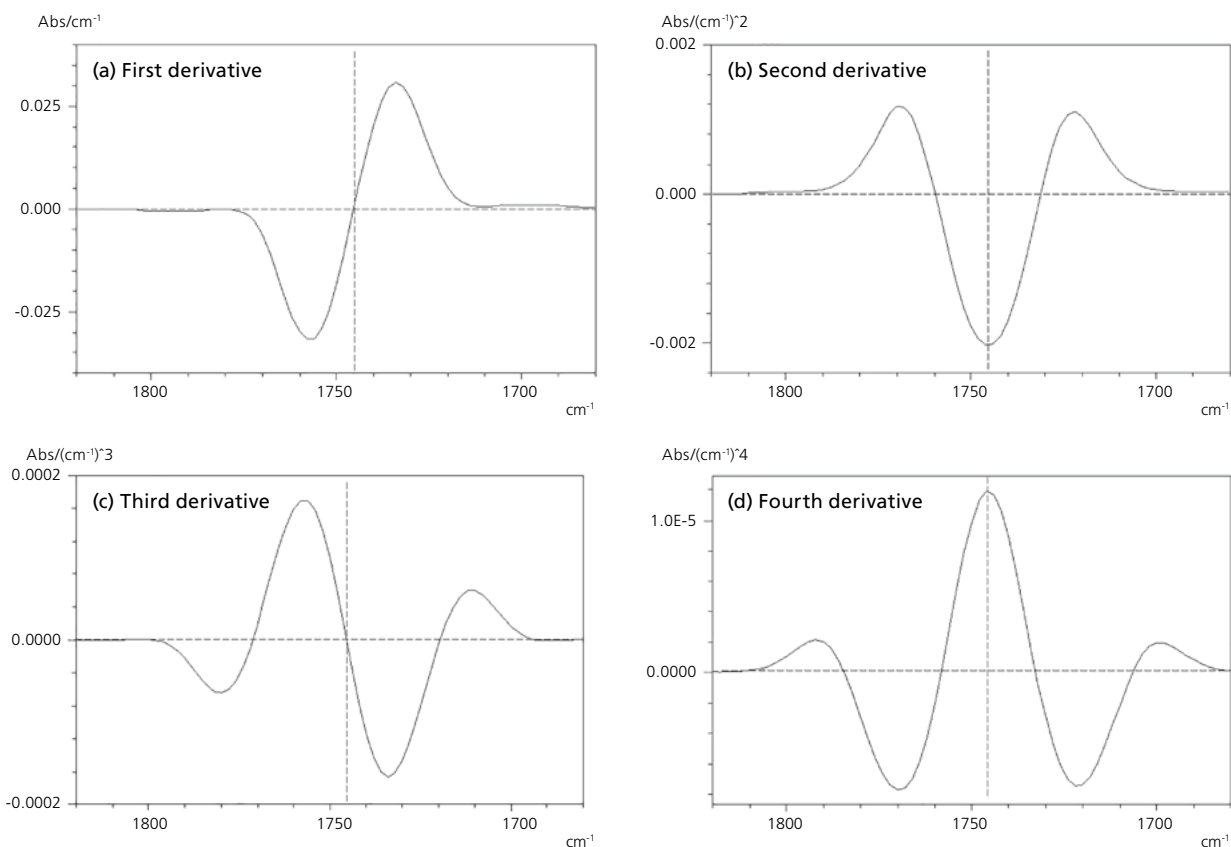


Fig. 4 Derivative Spectra of Vegetable Oil  
 (a) First derivative, (b) second derivative, (c) third derivative, and (d) fourth derivative spectra

### 3. Applications for Derivative Spectra

Three specific cases of using derivative spectra are described below.

#### 3-1. Data Analysis of UV-Degraded Plastics

Polyethylene terephthalate (PET) samples degraded with ultraviolet light were prepared as samples. Infrared spectra from the PET samples exposed to UV rays for 0 to 12 hours are shown in Fig. 5. They show that the longer the UV exposure, the more the peak near  $1,700\text{ cm}^{-1}$  shifted in the low-wavenumber direction, but it is difficult to compare any increases/decreases in peak intensity due to baseline fluctuations. Therefore, as shown in Fig. 6, first and second-order derivatives were calculated and baselines were aligned to make it easier to compare peak intensity increases/decreases. Baseline alignment improved with the first-derivative and increasingly the higher the derivative order level. That also enabled the wavenumber of broad peaks to be confirmed. Thus, slight peak variations can be clearly determined from derivative spectra.

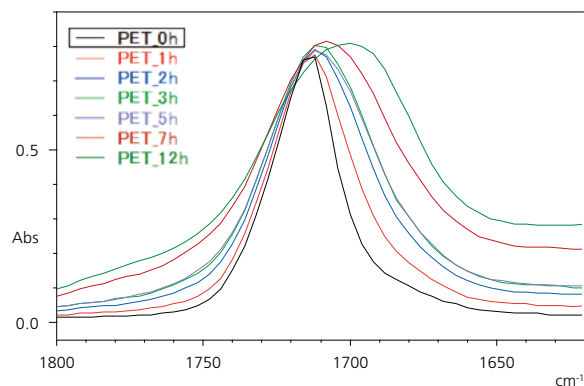


Fig. 5 Infrared Spectra of PET

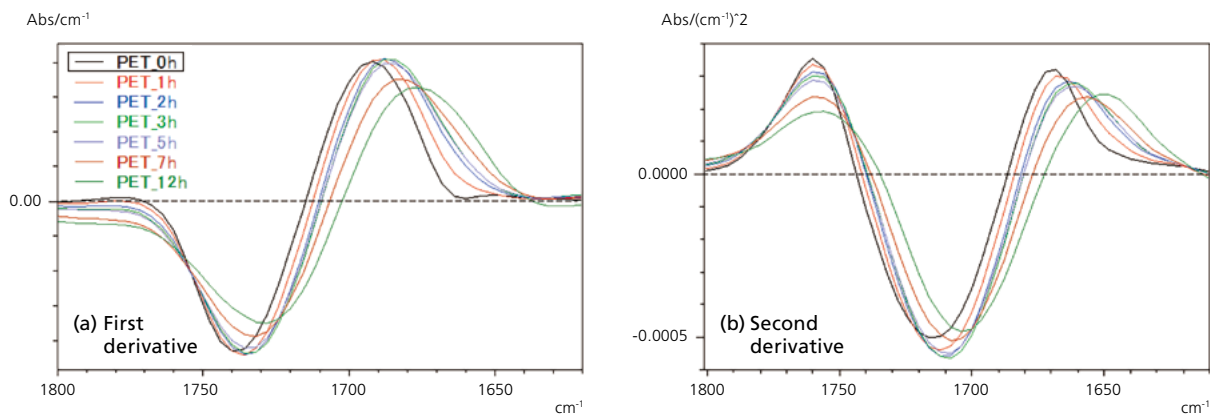


Fig. 6 Derivative Spectra of PET  
(a) First derivative and (b) second derivative spectra

### 3-2. Analysis of Secondary Protein Structures

Evaluating second-derivative spectra can also be useful for analyzing secondary structures of proteins (alpha-helix, beta-sheet, beta-turn, and random coil structures). Infrared spectra of proteins and other substances with high molecular weights and complex molecular structures can contain unseparated overlapping broad peaks due to multiple overlapping vibrations. In such cases, differentiation is useful for determining the correct position of peaks.<sup>[5]</sup>

In this case, the whites from chicken eggs were prepared as samples. Temperature was increased from 40 to 100 °C in 10 °C increments, with egg white samples dripped and measured after ensuring adequate heat transfer at each temperature. Fig. 7 shows the infrared spectra (amide I band) from the egg white samples, with corresponding second-derivative spectra of the egg white samples in Fig. 8. Though even the original infrared spectra show a difference, calculating the derivative clearly showed that the peaks can be clearly separated. Separating amide I band peaks requires first specifying the

position, number of fitted peaks, and other settings in advance. Those settings are determined from second and fourth-order derivative spectra.<sup>[5]</sup>

Details about that application were featured in Shimadzu Application News No. A592.

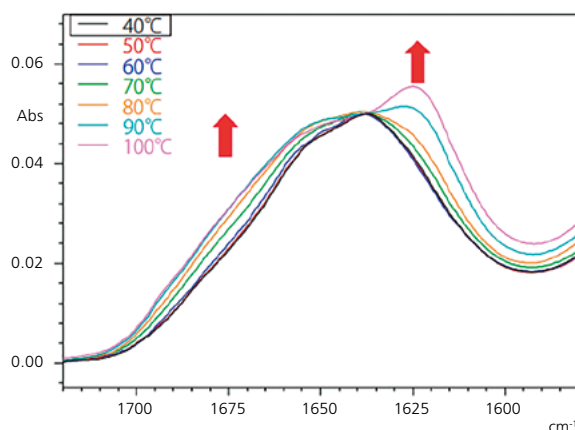


Fig. 7 Infrared Spectra of Egg Whites (Amide I Band)

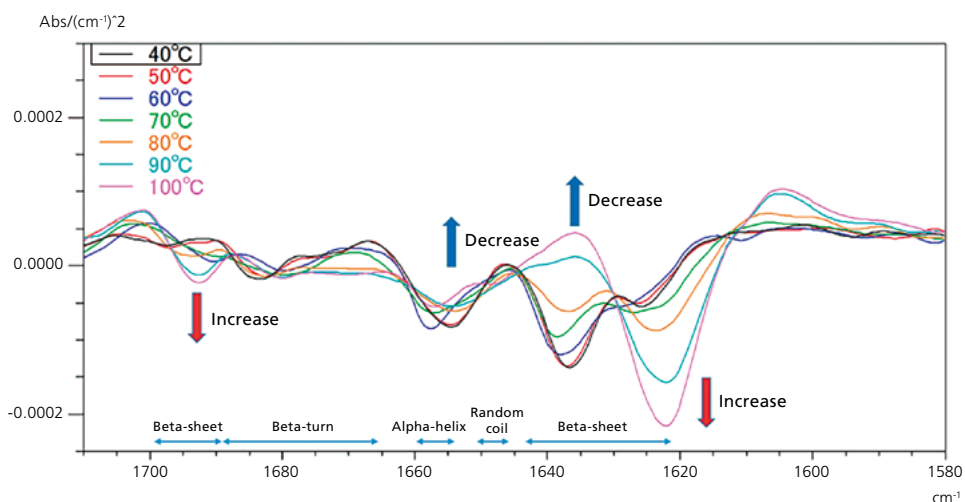


Fig. 8 Second-Derivative Spectra of Egg Whites (Amide I Band)

### 3-3. Characterization of SiO<sub>2</sub> Film on Silicon Wafer

It is difficult to perform quantitative calculations based on spectra with a fluctuating baseline. If that occurs, in some cases good results can be obtained by calculating the second-derivative spectrum and basing the quantitative calculations based on peak height.

In this example, the phosphorus (P), boron (B), and silicon (Si) content in a SiO<sub>2</sub> film applied on a silicon wafer was quantitated to evaluate the SiO<sub>2</sub> film properties. The infrared spectra

are shown in Fig. 9. These spectra were used for PLS quantitation. Representative true and predicted values for phosphorus (P) are indicated in Fig. 10. The coefficient of correlation  $r^2$  is 0.9769 for the original spectrum but 0.9908 for the second-derivative spectrum, which shows that the second-order differentiation provided superior results. Thus, it can be useful to calculate derivative spectra in advance as a pretreatment step before quantitative measurements, photometric measurements, or chemometric analysis such as PLS.

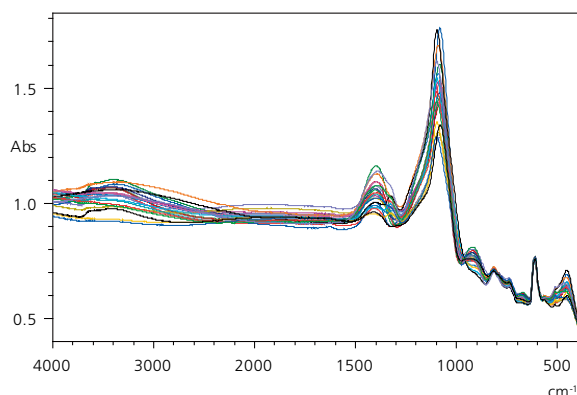


Fig. 9 Infrared Spectrum of SiO<sub>2</sub> Film on a Silicon Wafer

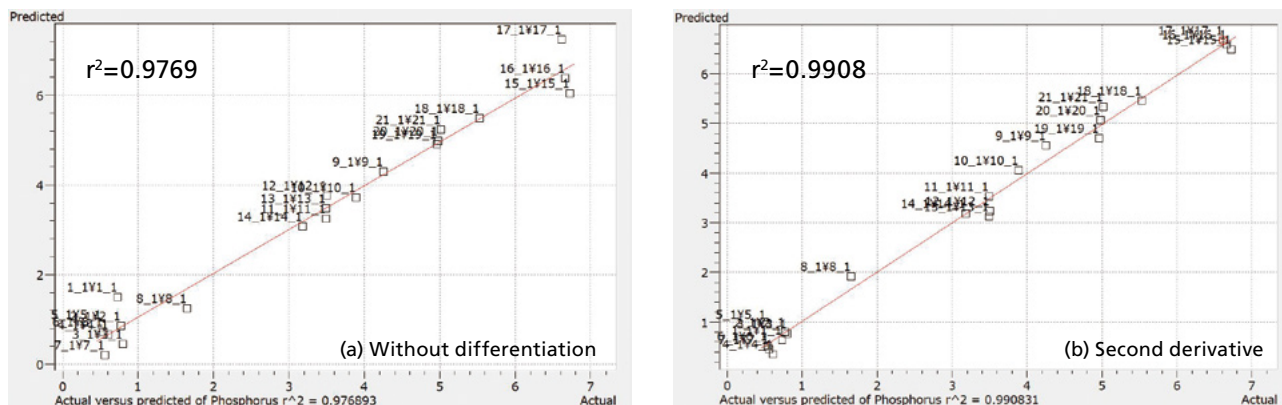


Fig. 10 True Value and Predicted Value of Phosphorus (P) Content  
(a) Without differentiation and (b) Second derivative

## 4. Summary

This article described an overview and features of derivative spectra and provided some application examples. Examples included analyzing UV-degraded plastics and the secondary structures of proteins, and PLS quantitative analysis of a SiO<sub>2</sub> film on a silicon wafer. To clearly show slight changes in peaks, to accurately determine peak positions, or to eliminate baseline fluctuations during PLS or other quantitative analysis, try calculating the derivative of spectra.

Note, however, that differentiation will increase noise levels, so the original infrared spectra must be of good quality. Therefore, selecting high-sensitivity FTIR analysis is recommended.

## References

- [1] A. Savitzky, M.J.E. Golay, *Anal. Chem.* 1964, 36(8), 1627-1639.
- [2] Shigeo Minami, *Spectral Data Processing for Scientific Measurement*, CQ Publishing (1986)
- [3] Kazuhiro Takahashi, *Journal of Surface Analysis*. 2000, 7(1), 68-77
- [4] Mitsuo Tasumi, *Fundamentals and Latest Techniques for Infrared Spectroscopy*, ST Japan (2012)
- [5] Hirotsugu Hiramatsu, *Secondary Structural Analysis Using Infrared Absorption Spectra*, Protein Science Society of Japan Archives (2009)

## Q&A

# What measurement method should I use to check the degradation of lubricant oil?

Reasons for lubricant oil degradation include oxidation, consumption of additives, and the build-up of sludge during use. Lubricant oil must be replaced at appropriate intervals because degradation can shorten equipment life or cause malfunctions.

The method for using FTIR to evaluate the degradation of lubricant oils is specified in ASTM E2412. That regulation specifies evaluating degradation based on the change in absorption level of infrared spectral measurements by the transmission method. Therefore, used and new lubricant oils were measured by the transmission method. Transmittance was measured using a Specac Pearl horizontal liquid transmittance measurement accessory shown in Fig. 1. The Pearl is a user-friendly accessory that can hold liquid

samples horizontally, inhibits bubble ingress, and is easier to clean than liquid cells typically used. Measurement results are shown in Fig. 2. Used lubricant oils tend to have higher absorption levels in the 3,500 to 3,150  $\text{cm}^{-1}$ , 1,750 to 1,700  $\text{cm}^{-1}$ , and 1,650 to 1,600  $\text{cm}^{-1}$  regions. Such changes in absorption are caused by contamination by water content or oxidation/nitration of the lubricant oil. Other components that can be measured by FTIR include sulfurized lubricant oils, contamination by gasoline or diesel fuels, soot ingress, and consumption of oxidation or wear inhibitors.

For more information about lubricant oils analysis, refer to Application News A603.



Fig. 1 Pearl Horizontal Liquid Transmission Measurement Accessory

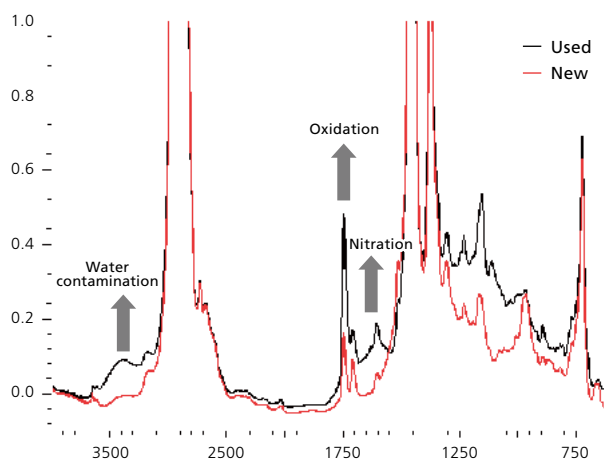
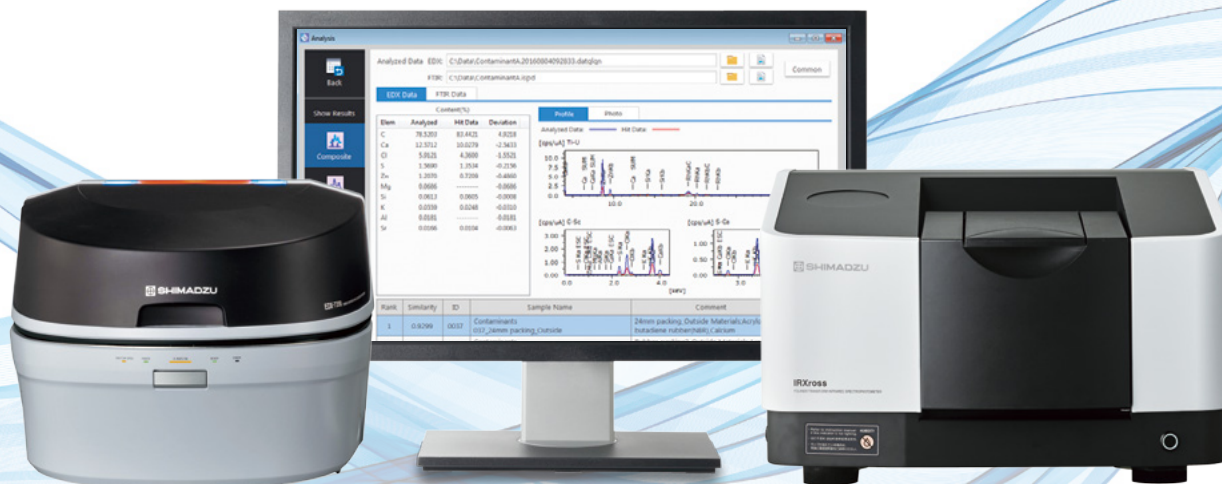


Fig. 2 Infrared Spectra of Lubricant Oil

# Shimadzu's Unique Integrated Analysis can Solve Problems with Contaminant Identification and Failure Analysis

Integrated EDX-FTIR Analysis Software EDXIR-Analysis



**NEW** EDX-7200

**NEW** IRXross

EDXIR-Analysis software is specially designed to perform qualitative analysis using data acquired by an energy dispersive X-ray (EDX) fluorescence spectrometer and a Fourier transform infrared spectrophotometer (FTIR). This software is used to perform an integrated analysis of data from FTIR, which is excellent at the identification and qualification of organic compounds, and from EDX, which is excellent at the elementary analysis of metals, inorganic compounds and other content. It then pursues identification results and the degree of matching.

For more details, click here.

<https://www.shimadzu.com/an/products/molecular-spectroscopy/ftir/ftir-spectroscopy/edxir-analysis-contaminant-findermaterial-inspector/index.html>



Provides High-Speed Response and High Stability  
New automatic door functionality makes weighing operations even more convenient

Advanced Performance UniBloc Balances

## AP W-AD Series



For more details, click here.

<https://www.shimadzu.com/an/products/balances/analytical-balances/ap-series/index.html>



Shimadzu Corporation  
[www.shimadzu.com/an/](http://www.shimadzu.com/an/)

**For Research Use Only. Not for use in diagnostic procedures.**

This publication may contain references to products that are not available in your country. Please contact us to check the availability of these products in your country. Company names, products/service names and logos used in this publication are trademarks and trade names of Shimadzu Corporation, its subsidiaries or its affiliates, whether or not they are used with trademark symbol "TM" or "®". Third-party trademarks and trade names may be used in this publication to refer to either the entities or their products/services, whether or not they are used with trademark symbol "TM" or "®". Shimadzu disclaims any proprietary interest in trademarks and trade names other than its own.

The contents of this publication are provided to you "as is" without warranty of any kind, and are subject to change without notice. Shimadzu does not assume any responsibility or liability for any damage, whether direct or indirect, relating to the use of this publication.